

## Analysis of partially embedded beams in two-parameter foundation

A.Yalçın Akoz<sup>1a</sup> and Hale Ergun<sup>\*2</sup>

<sup>1</sup>Engineering Faculty, Civil Engineering Department, T.C. Maltepe University, Istanbul, Turkey

<sup>2</sup>Civil Engineering Faculty, Civil Engineering Department, ITU, Istanbul, Turkey

(Received June 18, 2011, Revised December 20, 2011, Accepted February 21, 2012)

**Abstract.** In this study, Pasternak foundation model, which is a two parameter foundation model, is used to analyze the behavior of laterally loaded beams embedded in semi-infinite media. Total potential energy variation of the system is written to formulate the problem that yielded the required field equations and the boundary conditions. Shear force discontinuities are exposed within the boundary conditions by variational method and are validated by photo elastic experiments. Exact solution of the deflection of the beam is obtained. Both foundation parameters are obtained by self calibration for this particular problem and loading type in this study. It is shown that, like the first parameter  $k$ , the second foundation parameter  $G$  also depends not only on the material type but also on the geometry and the loading type of the system. On the other hand, surface deflection of the semi infinite media under singular loading is obtained and another method is proposed to determine the foundation parameters using the solution of this problem.

**Keywords:** Pasternak foundation; variational method; photo elastic method; experimental method for Pasternak constants; boundary conditions; sub grade; two parameter foundation

---

### 1. Introduction

Laterally loaded beams embedded in semi-infinite media is a common problem that can be used to model a variety of applications in engineering, dentistry and even orthopedics; such as structure foundation members, piles, rails, pipelines, fibers in composites, implants, to name a few. The origin of the solution to this problem may be traced back to Winkler's foundation model developed for rails (Hetenyi 1946). Foundation models in literature can be classified within two basic classical approaches as Winklerian and Continuum models. Winkler model acts as if it consisted of infinitely many closely spaced linear springs, where only one parameter  $k$ , which is subgrade modulus, characterizes the behavior of the foundation. Interactions between springs are not considered, so it does not accurately represent the characteristics of many practical foundations (Zhaohua and Cook 1983, Alemdar and Gulkan 1999, Civalek 2007). Pasternak model is an improved Winklerian approach that is modified to introduce continuity through interaction amongst the spring elements

---

\*Corresponding author, Assistant Professor, E-mail: [ergunh@itu.edu.tr](mailto:ergunh@itu.edu.tr)

<sup>a</sup>Professor, E-mail: [y.akoz@ttmail.com](mailto:y.akoz@ttmail.com), [yakoz@maltepe.edu.tr](mailto:yakoz@maltepe.edu.tr)

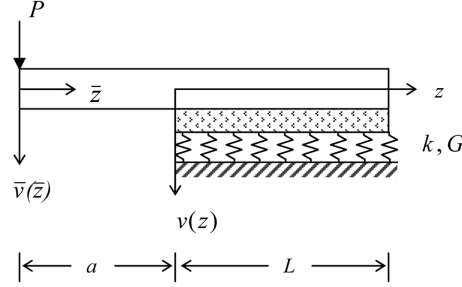


Fig. 1 The geometry of the problem and Pasternak foundation model

(Dutta and Roy 2002), where both  $k$  and a second parameter  $G$ , which is shear modulus, characterize the behavior of the foundation.

Finite element method is the most popular one among the solution methods considered to analyze the problem, but it is time consuming to obtain the parametrical results with this method. In order to understand the characteristic behavior of the beam, we need to study the parametric relations that can be obtained from a theoretical solution.

In this study, the media that the elastic beam is embedded is modeled as Pasternak foundation (Fig. 1). Field equations and boundary conditions of the problem will be determined using energy and variation methods. Implicit closed solutions will be presented where the parameters of the problem are clearly identified and easy to follow.

The most important distinctive property of the Pasternak foundation model is that it exposes the discontinuity of the shear resultant force at the point where the beam enters the media. This discontinuity can only be exposed with the Pasternak foundation model and can easily be obtained within the variational method (Gelfand and Fomin 1963, Kerr 1976). If the second parameter is set to zero, the formulas of the two-parameter Pasternak foundation model reduce to those of the one-parameter Winkler foundation model, which is a special case of Pasternak foundation model. To check the results, the same solutions are obtained with Winkler foundation for engineering purposes, but the discontinuity in the shear resultant force could not be obtained as expected.

We should emphasize two important points of this study. First, discontinuity of shear force is obtained theoretically and validated by photo elastic experiments. Second, the method is proposed to obtain the second parameter  $G$  and this method is used to solve this specific problem. This method can be easily applied to similar problems to obtain  $G$ .

## 2. Pasternak foundation model

In this section, the behavior of a laterally loaded beam embedded in a semi-infinite plane is studied using the Pasternak foundation model (Fig. 1). Here,  $v(z)$  is the deflection of the beam section along the embedded length  $L$  and  $\bar{v}(\bar{z})$  is the deflection of the beam section along the cantilever beam length  $a$  as shown in Fig. 1.

Total potential energy  $\Pi$  of the beam can be written as follows.

$$\Pi = \int_0^a \frac{EI}{2} (\bar{v}'')^2 d\bar{z} - P\bar{v}(0) + \int_0^L \frac{EI}{2} (v'')^2 dz + \int_0^L \left( \frac{G}{2} (v')^2 + \frac{k}{2} v^2 \right) dz \quad (1)$$

Where,  $EI$  is the flexural rigidity of the beam. The first parameter  $k$  and the second parameter  $G$  of the Pasternak foundation model have units N/mm/mm and N, respectively. The variation of the total potential energy  $\delta\Pi$  can be written as follows. Here,  $\delta$  prefix is to denote the arbitrary variation of the variable.

$$\delta\Pi = \int_0^a EI\bar{v}'' \delta\bar{v}'' d\bar{z} - P\delta\bar{v}(0) + \int_0^L EIv'' \delta v'' dz + \int_0^L (Gv' \delta v' + kv\delta v) dz = 0$$

After applying required partial integrations, following equation can be obtained.

$$\begin{aligned} \delta\Pi = & EI\bar{v}'' \delta\bar{v}'|_0^a - EI\bar{v}''' \delta\bar{v}|_0^a + \int_0^a EI\bar{v}^{IV} \delta\bar{v} d\bar{z} + EIv'' \delta v'|_0^L - EIv''' \delta v|_0^L + Gv' \delta v|_0^L \\ & + \int_0^L (EIv^{IV} - Gv'' + kv) \delta v dz - P\delta\bar{v}(0) = 0 \end{aligned} \quad (2)$$

The beam enters the medium at  $\bar{z} = a$  and  $z = 0$ , which is named as transition section in this study. In order to complete the formulation of the problem, the continuity of the beam and its variations at the transition section should be written as follows.

$$\left. \begin{aligned} \bar{v}(a) &= v(0) \\ \bar{v}'(a) &= v'(0) \end{aligned} \right\} \Rightarrow \left. \begin{aligned} \delta\bar{v}(a) &= \delta v(0) \neq 0 \\ \delta\bar{v}'(a) &= \delta v'(0) \neq 0 \end{aligned} \right\} \quad (3)$$

According to the variational theorem (Gelfand and Fomin 1963, Kerr 1976), since the variations of the variables are arbitrary, the integrands in Eq. (2) must be equal to zero as follows.

$$\begin{aligned} \bar{v}^{IV} \delta\bar{v} &= 0 & 0 < \bar{z} < a \\ (v^{IV} - 2\eta^2 v'' + \lambda^4 v) \delta v &= 0 & 0 < z < L \end{aligned} \quad (4)$$

Here,  $\lambda$  and  $\eta$  are defined as in Eqs. (5a-b).

$$\lambda^4 = k/EI \quad (5a)$$

$$2\eta^2 = G/EI \quad (5b)$$

Also from Eq. (2), the following equation can be written.

$$\begin{aligned} & [-EI\bar{v}''(0)] \delta\bar{v}'(0) + [EI\bar{v}'''(0) - P] \delta\bar{v}(0) + [EIv''(L)] \delta v'(L) \\ & + [EI\bar{v}''(a) - EIv''(0)] \delta v'(0) + [Gv'(L) - EIv'''(L)] \delta v(L) \\ & + [EIv'''(0) - EI\bar{v}'''(a) - Gv'(0)] \delta\bar{v}(0) = 0 \end{aligned} \quad (6)$$

The field equations of the problem can be written as follows.

$$\bar{v}^{IV} = 0 \quad 0 < \bar{z} < a \quad (7a)$$

$$v^{IV} - 2\eta^2 v'' + \lambda^4 v = 0 \quad 0 < z < L \quad (7b)$$

Boundary conditions are written as follows.

$$\bar{v}''(0) = 0 \quad (8a)$$

$$-EI\bar{v}'''(0) = -P \quad (8b)$$

$$\bar{v}''(a) = v''(0) \quad (8c)$$

$$-EIv'''(0) + EI\bar{v}'''(a) = -Gv'(0) \quad (8d)$$

$$v''(L) = 0 \quad (8e)$$

$$-EIv'''(L) = -Gv'(L) \quad (8f)$$

To be able to complete the problem, the continuity of the displacement and the rotation at the transition point must be added to the boundary conditions as follows.

$$\bar{v}(a) = v(0) \quad (8g)$$

$$\bar{v}'(a) = v'(0) \quad (8h)$$

Finally, the problem is mathematically expressed with two differential governing equations Eqs. (7a-b) and eight boundary conditions Eqs. (8a-h). The solution of Eq. (7a), which is in the interval  $0 < \bar{z} < a$ , is given as follows.

$$\bar{v}(\bar{z}) = \delta_o + \theta_o \bar{z} + \frac{P}{6EI} \bar{z}^3 \quad (9)$$

Where,  $\delta_o$  and  $\theta_o$  are the displacement and the rotation at  $\bar{z} = 0$ , respectively. For the solution of the differential equation given in Eq. (7b), the proposed form  $v = \exp(pz)$  yields three conditions according to the characteristic equation roots which depend on the material constants  $\eta$  and  $\lambda$ . Two cases, which are  $\eta = \lambda$  and  $\eta > \lambda$ , are rarely encountered in applications. General solutions for both are given here, but the boundary conditions are not studied. These cases are discussed by Gulkan and Alemdar (1999) in detail.

General solutions for  $\eta = \lambda$  and  $\eta > \lambda$  are given below in Eq. (10) and Eq. (11) respectively.

$$v(z) = C_1 e^{\lambda z} + C_2 z e^{\lambda z} + C_3 e^{-\lambda z} + C_4 z e^{-\lambda z} \quad (10)$$

$$v(z) = D_1 e^{\mu_1 z} + D_2 e^{-\mu_1 z} + D_3 e^{\mu_2 z} + D_4 e^{-\mu_2 z} \quad (11)$$

Where,  $\mu_1$  and  $\mu_2$  are defined as follows.

$$\mu_1^2 = \eta^2 + \sqrt{\eta^4 - \lambda^4}$$

$$\mu_2^2 = \eta^2 - \sqrt{\eta^4 - \lambda^4}$$

The third condition is  $\eta < \lambda$  that is common in the applications. The characteristic equation can be written for this case as follows.

$$\begin{aligned}
p^2 &= \eta^2(1 \mp i\sqrt{\varphi-1}) \\
p^2 &= \eta^2\sqrt{\varphi}\exp(\mp 2i\theta)
\end{aligned} \tag{12}$$

Where

$$\begin{aligned}
\cos 2\theta &= 1/\sqrt{\varphi} \\
\sin 2\theta &= \sqrt{\varphi-1}/\sqrt{\varphi}
\end{aligned} \tag{13}$$

New material constants  $\kappa$  and  $\varphi$  are defined in terms of old material constants  $\eta$  and  $\lambda$  as follows.

$$\begin{aligned}
\kappa &= \eta^2\sqrt{\varphi-1} \\
\varphi &= \lambda^4/\eta^4
\end{aligned} \tag{14}$$

The characteristic equation can be rewritten using the trigonometric relations in Eq. (13) as follows.

$$p_{nk} = (-1)^n \lambda \exp(i\theta(-1)^k) \quad n, k = 0, 1 \tag{15}$$

We define  $\alpha$  and  $\beta$  in terms of  $\lambda$  and  $\theta$  as follows.

$$\alpha = \lambda \cos \theta \tag{16a}$$

$$\beta = \lambda \sin \theta \tag{16b}$$

The following relations exist between the constants those which significantly facilitate the calculations.

$$\begin{aligned}
\alpha^2 + \beta^2 &= \lambda^2 \\
\alpha^2 - \beta^2 &= \eta^2 \\
2\alpha\beta &= \lambda^2 \sin 2\theta \\
3\alpha^2 - \beta^2 - 2\eta^2 &= \lambda^2 \\
3\beta^2 - \alpha^2 + 2\eta^2 &= \lambda^2
\end{aligned} \tag{17}$$

Solution of the differential Eq. (7b) can be written as follows for this condition.

$$v(z) = (A+C)K11 + (B+D)K12 + (A-C)K21 + (B-D)K22 \tag{18a}$$

This solution is the one that represents the physics of the problem considered in this study. To be able to apply the boundary conditions, the higher differential expressions of the solution are presented as follows.

$$\begin{aligned}
v'(z) &= (A+C)[\alpha K21 - \beta K12] + (A-C)[\alpha K11 - \beta K22] \\
&+ (B+D)[\alpha K22 + \beta K11] + (B-D)[\alpha K12 + \beta K21]
\end{aligned} \tag{18b}$$

$$v''(z) = (A+C)[\eta^2 K11 - \kappa K22] + (A-C)[\eta^2 K21 - \kappa K12] \\ + (B+D)[\eta^2 K12 + \kappa K21] + (B-D)[\eta^2 K22 + \kappa K11] \quad (18c)$$

$$v'''(z) = (A+C)[\alpha F1 K21 - \beta F2 K12] + (A-C)[\alpha F1 K11 - \beta F2 K22] \\ + (B+D)[\alpha F1 K22 + \beta F2 K11] + (B-D)[\alpha F1 K12 + \beta F2 K21] \quad (18d)$$

Here,  $KIJ$  ( $I, J = 1, 2$ ) are the functions of  $z$  given as follows.

$$K11 = ch(\alpha z) \cos(\beta z) \\ K12 = ch(\alpha z) \sin(\beta z) \\ K21 = sh(\alpha z) \cos(\beta z) \\ K22 = sh(\alpha z) \sin(\beta z) \quad (19)$$

Here,  $F1$  and  $F2$  are defined as follows.

$$F1 = 2\eta^2 - \lambda^2 \\ F2 = 2\eta^2 + \lambda^2 \quad (20)$$

The solution  $v(z)$  given in Eq. (18a) and the solution  $\bar{v}(\bar{z})$  given in Eq. (9) have six unknown constants as  $A, B, C, D, \delta_o$  and  $\theta_o$ . Using four boundary Eqs. (8c-f) and two continuity conditions Eqs. (8g-h), problem is reduced to two equations and written in the matrix form as follows.

$$\begin{bmatrix} A11 & A12 \\ A21 & A22 \end{bmatrix} \begin{Bmatrix} \delta_o \\ \theta_o \end{Bmatrix} = \begin{Bmatrix} B1 \\ B2 \end{Bmatrix} \quad (21)$$

Where,  $AIJ$  and  $BJ$  ( $I, J = 1, 2$ ) constants are given as follows.

$$A11 = M1 - \frac{\eta^2 M3}{\kappa} \\ A12 = aM1 + \frac{M2}{2\alpha} - \frac{a\eta^2 M3}{\kappa} + \frac{M4}{2\beta} \\ A21 = M6 - \frac{\eta^2 M8}{\kappa} \\ A22 = aM6 + \frac{M5}{2\alpha} - \frac{a\eta^2 M8}{\kappa} + \frac{M7}{2\beta} \\ B1 = -\frac{Pa^2}{EI} \left( \frac{aM1}{6} - \frac{M2}{2\alpha a^2 \lambda^2} + \frac{M2}{4\alpha} + \frac{M3}{\alpha \kappa} - \frac{a\eta^2 M3}{6\kappa} + \frac{M4}{4\beta} + \frac{M4}{2\beta a^2 \lambda^2} \right) \\ B2 = -\frac{Pa^2}{EI} \left( \frac{aM6}{6} + \frac{M7}{2\beta a^2 \lambda^2} + \frac{M7}{4\beta} + \frac{M8}{\alpha \kappa} - \frac{a\eta^2 M8}{6\kappa} + \frac{M5}{4\alpha} - \frac{M5}{2\alpha a^2 \lambda^2} \right) \quad (22)$$

Where,  $MJ$  ( $J = 1, \dots, 8$ ) constants are given as follows.

$$\begin{aligned}
M1 &= \eta^2 \bar{K}11 - \kappa \bar{K}22 \\
M2 &= \eta^2 \bar{K}21 - \kappa \bar{K}12 \\
M3 &= \eta^2 \bar{K}22 + \kappa \bar{K}11 \\
M4 &= \eta^2 \bar{K}12 + \kappa \bar{K}21 \\
M5 &= \alpha \bar{K}11 + \beta \bar{K}22 \\
M6 &= \alpha \bar{K}21 + \beta \bar{K}12 \\
M7 &= \alpha \bar{K}22 - \beta \bar{K}11 \\
M8 &= \alpha \bar{K}12 - \beta \bar{K}21
\end{aligned} \tag{23}$$

Where,  $\bar{K}_{IJ}$  constants are the values of  $K_{IJ}$  functions at  $z = L$ . After solving the linear system of equation in Eq. (21),  $\delta_o$  and  $\theta_o$  can be determined. Thus, the expressions for the deflection, slope, bending moment, transverse shear force and distributed foundation reaction along the beam can be calculated.

### 3. Material constants

Foundation parameters are used as input data to analyze the structure foundation interaction in numerous studies in literature, thus a study on the determination of the foundation parameters is extensively favorable. Experimental and/or computational studies are mostly limited only to the first parameter of the foundation (Kobayashi *et al.* 2008, Kim and Jeong 2011, ASTM 1998). Material constants  $k$  and  $G$  depend not only on the material but on geometry and loading type as well (Dutta 2002, Setiadji 2009). To show that  $k$  depends on both geometry and material constant, we consider a tensile bar of length  $L$ , cross sectional area  $A$  and material constant  $E$ , subjected to load  $P$ . Extension of the bar is calculated as  $\Delta = (L/EA)P$  where coefficient of  $P$  is known as  $1/K$ , i.e.,  $K = EA/L$ . Since  $E$  is a fundamental material property, there are several theoretical and experimental studies to obtain the relationship between  $k$  and the Elastic modulus in literature (Bowles 1974, Setiadji and Fwa 2009, Dinçer 2011).

In this section, the problem of the deflection  $v$  of the semi-infinite plate boundary subjected to a singular load  $P$  is considered and it is aimed to determine the material constants, which are the parameters of Pasternak foundation. The problem is depicted in Fig. 2.

The total potential energy  $\Pi$  of the system can be written as follows.

$$\Pi = 2 \int_0^\infty \left( \frac{G}{2} (v')^2 + \frac{k}{2} v^2 \right) dz - P v(0) \tag{24}$$

Where,  $v_o$  is the deflection at the point where singular load  $P$  is applied. The variation of the total potential energy can be written as follows.

$$\delta \Pi = 2 \int_0^\infty (G v' \delta v' + k v \delta v) dz - P \delta v(0) = 0 \tag{25}$$

After the application of the required partial integrations, the following expression is obtained.

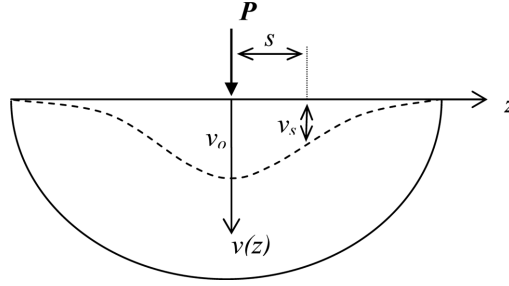


Fig. 2 The schematic drawing of singular loading experiment

$$\delta\Pi = 2 \int_0^{\infty} (kv - Gv'') \delta v dz + 2Gv'(\infty) \delta v(\infty) - [2Gv'(0) + P] \delta v(0) \quad (26)$$

According to the fundamental principles of the variational theorem, the multipliers must be equal to zero, since the variations of variables are arbitrary (Gelfand and Fomin 1963). Thus, in the field, the following governing equation can be written.

$$v'' - \omega^2 v = 0 \quad 0 < z < \infty \quad (27)$$

Where,  $\omega^2 = k/G$ . And at the boundaries, the following conditions can be written.

$$v' = -P/2G \quad z = 0 \quad (28a)$$

$$v' = 0 \quad z = \infty \quad (28b)$$

The solution of the differential equation Eq. (27), after applying the boundary conditions Eqs. (28a-b), can be determined as follows.

$$v(z) = \frac{Pe^{-\omega z}}{2G\omega} \quad (29)$$

Suppose that the deflections at  $z = 0$  and  $z = s$  points are measured as  $v_o$  and  $v_s$  respectively as shown in Fig. 2. From the substitution of these two conditions in Eq. (29),  $k$  and  $G$  parameters can be found as follows.

$$k = \frac{P \ln(v_o/v_s)}{2v_o s} \quad (30a)$$

$$G = \frac{Ps}{2v_o \ln(v_o/v_s)} \quad (30b)$$

For simpler expressions, besides the measured  $v_o$  deflection, if the distance  $s_e$  is measured provided that the relation  $e = v_o/v_s$  is met, where  $e$  is Euler's constant, Eqs. (30a-b) can be rewritten as follows.

$$k = \frac{P}{2v_o s_e} \quad (31a)$$



$$G = \frac{Ps_e}{2v_o} \quad (31b)$$

Solving Eqs. (31a) and (31b), relation between  $G$  and  $k$  is as follows.

$$G = ks_e^2 \quad (32)$$

#### 4. Self calibration and experimental verification

To be able to check the mathematical model and verify the solutions, we have it found beneficial and complementary to appeal to the photo elastic experiments. The beam and the media were represented by a polymer plate of 0.5 cm thickness. The beam was  $h = 2$  cm in height and 16 cm in length. The embedded length of the beam was  $L = 6$  cm, and the beam distances from the transition section to the point where the lateral load  $P = 39$  N applied at the outside of the foundation were chosen to be  $a = 3$  cm,  $a = 6$  cm and  $a = 9$  cm.

Stress-optic law of photo elasticity in two dimensions is  $\sigma_1 - \sigma_2 = n f / t$ , where  $\sigma_i$  are the principal stresses,  $t$  is the thickness of the model and  $n$  is the fringe order. When a loaded transparent model is placed in the field of a standard circular polariscope, bands of equal colors in the stress pattern appear those are known as fringes. Starting from black, with every repeat of complete rainbow colors, fringe order counts one more on zero value. Due to stress optic law, a fringe is the locus of points of constant difference between the principal stresses. Thus, at isotropic and singular points  $\sigma_1 = \sigma_2$ , the fringe order value is zero and black colored in the pictures (Frocht 1941).

A preliminary experiment, which was a four point bending test, was conducted on the polymer beam and the Elastic modulus was measured as  $E = 2.7$  GPa and the stress-optic constant was measured as  $f = 134$  N/cm/fringe approximately.

Three isocromatic pictures are shown in Fig. 3 for three models which are subjected to the same load  $P = 39$  N. To interpret the isotropic points on these pictures, it is helpful to draw the free body

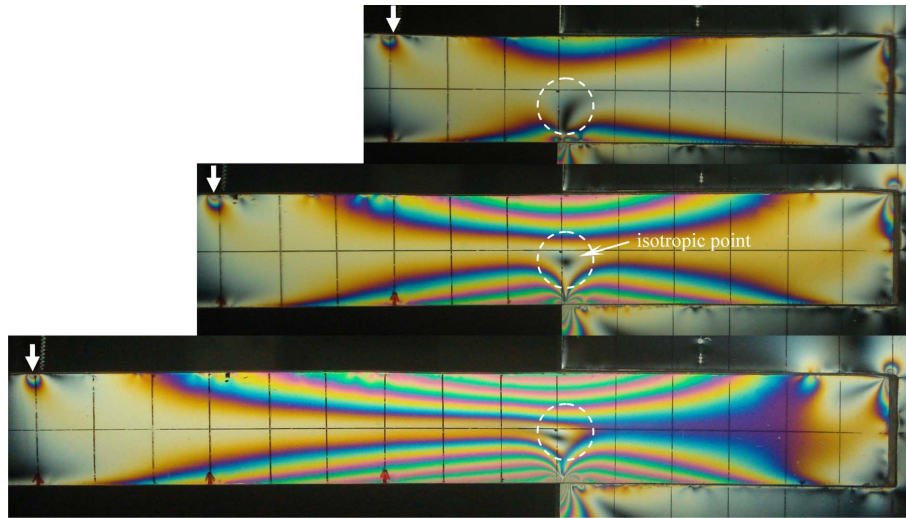


Fig. 3 Photo elastic experiments conducted for  $P = 39$  N,  $L = 6$  cm, (a)  $a = 3$  cm, (b)  $a = 6$  cm, (c)  $a = 9$  cm

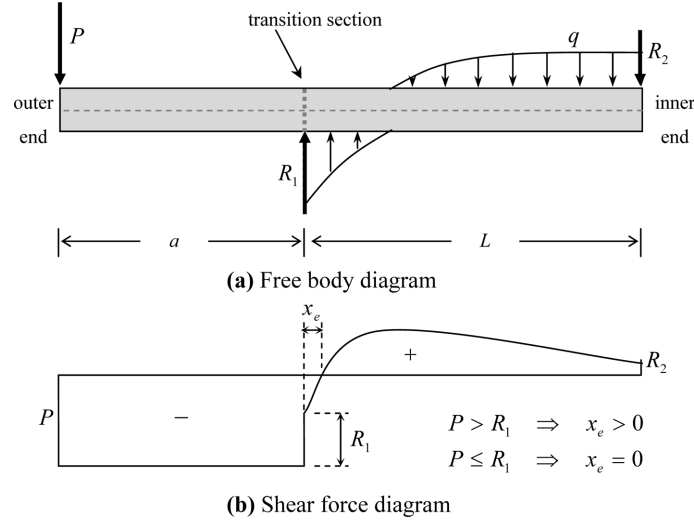


Fig. 4 (a) Free body diagram, (b) Shear force diagram

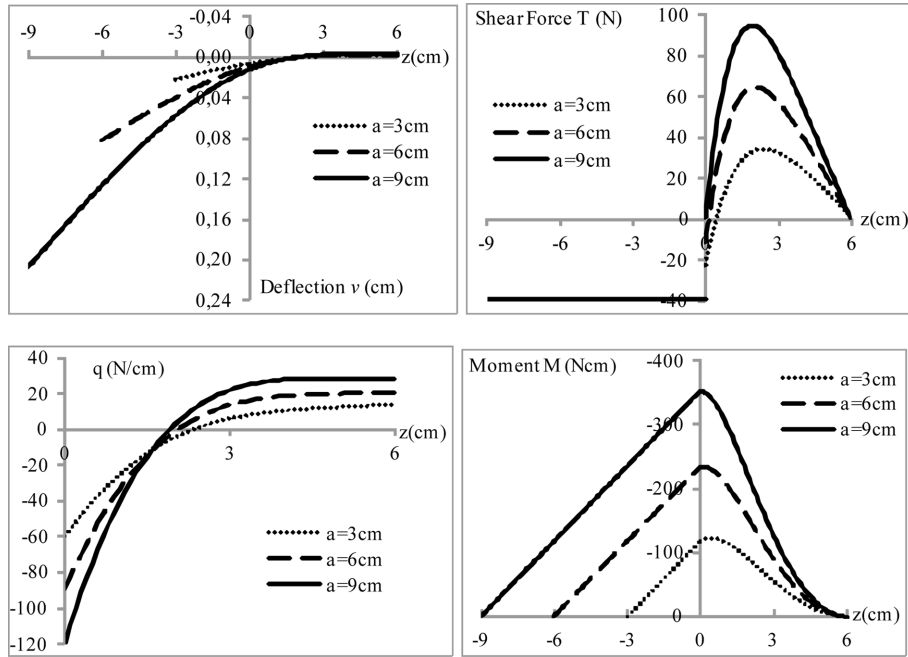


Fig. 5 Deflection, shear force, moment and distributed foundation reaction force diagrams for all loading cases

and shear force diagrams as shown in Fig. 4(a-b).

To calculate material constants  $k$  and  $G$ , two measurements are necessary.

In the first experiment, at the outer end point where the load  $P$  is applied, the deflection  $\delta_o$  of the beam is measured approximately as 2 mm for  $a = 9$  cm. A program is written in Mathematica to computerize the theory developed in this study. Using this program,  $k = 0.1$  GPa is found to provide

Table 1 Program output for all loading cases using  $k = 0.1$  GPa and  $G = 4$  kN parameter values

$a$ (cm)	$\delta_o$ (cm)	$\theta_o$ (cm)	$\delta_1$ (cm)	$\theta_1$ (cm)	$T_1$ (N)
9	0.208	-0.0275	0.0135	-0.0099	0.876
6	0.083	-0.0148	0.0100	-0.0070	-10.86
3	0.023	-0.0060	0.0060	-0.0040	-22.59

$\delta_o = 2$  mm.

To obtain  $G$ , the photo elastic experiments are used. Observation of isotropic points in all experiments shown in Fig. 3 denotes the presence of singular reaction force acting to the beam (Frocht 1941) at the transition point. In the third experiment for  $a = 9$  cm,  $P = 39$  N, it is observed that  $x_e = 0$ , at the same time  $R_1 = P$  at the transition section which corresponds to  $T_1 = 0$ . Here,  $R_1$  is the singular reaction force that is obtained with the boundary condition in Eq. (8d),  $x_e$  is the distance between the transition section and the isotropic point location as shown in Fig. 4(b),  $T_1$  is the transverse shear force value at the embedded side of the transition point.  $G = 4$  kN is found to verify this result in the Mathematica program.

Using these parameter values, deflection, shear force, moment and distributed reaction force diagrams for all loading cases  $a = 9$  cm,  $a = 6$  cm and  $a = 3$  cm are plotted in Fig. 5. In this figure, positive z-axis in the diagrams corresponds to the embedded region of the beam. Also the results are given in Table 1, where  $\delta_1$  and  $\theta_1$  are the displacement and rotation of the beam at the transition point ( $z = 0$ ), respectively. When these diagrams are examined, it can be seen that the characteristic results observed in experiments are compatible with the theoretical solutions.

## 5. Conclusions

In this study, to obtain the effects of the laterally loaded beam on the foundation, instead of inspecting the foundation, the beam, which is easier to analyze, is examined. The elastic media is modeled as Pasternak foundation.

The field equations and the boundary conditions are obtained by variation of the system total potential energy. This method is very important especially to obtain the realistic boundary conditions. Also the field equations can be determined very easily.

The solution is obtained in terms of Pasternak foundation constants  $G$ ,  $k$  and the flexural rigidity  $EI$  for three different cases.

Good agreement with the solutions obtained from the mathematical model and the ones from the experiments confirms the validity of the simple model proposed in this study. The advantages resulted from the cooperation of using both the experiment and the theory together must be emphasized again with this occasion.

As a result following three results can be extracted:

- One of the most significant results of this study is that shear force discontinuities are exposed by variational method and validated by photo elastic experiments. This is generally overlooked in similar problems in literature.
- It is shown that Pasternak parameter  $G$  depends not only on the material but also on geometry and loading type, maybe that is why it is hard to find  $G$  parameters of foundations in literature. The other important issue is that parameter  $G$  for the media is determined by self calibration. And

the theoretical result is obtained for this particular model and loading type. This method can be applied to similar problems.

- Deflection function of the semi-infinite media subjected to a concentrated load  $P$  is obtained. Using this function, a method that can be used to determine  $G$  and  $k$  parameters of the foundation is proposed (Fig. 2).

## Acknowledgements

The authors are motivated with the need to solve the problem in implant applications that were experienced by Prof. Dr. Cetin Sevuk, Dr. Zeynep Sevuk and Dr. Anla Akata who are the members of Dentistry Faculty of CAPA, Istanbul, Turkey. The photo elastic experiments were conducted in ITU Experimental Mechanics Laboratory, Istanbul, Turkey. The background of this study was discussed at 16th National Mechanics Conference, Erciyes University, Kayseri, Turkey on June 22-26, 2009, in Turkish and improved to be published.

## References

- Akoz, A.Y. and Ergun, H. (2009), "Implants and Pasternak foundation", *Proceeding of the 16th National Mechanics Congress*, Erciyes University, Kayseri, Turkey, June. (in Turkish)
- American Society of Testing and Materials (1998), "Standard test method for repetitive static plate load tests of soils and flexible pavement components, for use in evaluation and design of airport and highway pavements" (D1195-93), 04.08, 110-113.
- Bowles, J.E. (1974), *Analytical and Computer Methods in Foundation Eng*, Mc Graw-Hill.
- Civalek, O. (2007), "Nonlinear analysis of thin rectangular plates on Winkler-Pasternak elastic foundations by DSC-HDQ methods", *Appl. Math. Model.*, **31**(3), 606-624.
- Dinçer, İ. (2011), "Models to predict the deformation modulus and the coefficient of subgrade reaction for earth filling structures", *Adv. Eng. Softw.*, **42**, 160-171.
- Dutta, S.C. and Roy, R. (2002), "A critical review on idealization and modeling for interaction among soil-foundation-structure system", *Comput. Struct.*, **80**, 1579-1594.
- Frocht, M.M. (1941), *Photoelasticity*, Vol.I, John Wiley & Sons Inc.
- Gelfand, I.M. and Fomin, S.V. (1963), *Calculus of Variations*, Prentice-Hall Inc.
- Gulkan, P. and Alemdar, B.N. (1999), "An exact finite element for a beam on a two-parameter elastic foundation: a revisit", *Struct. Eng. Mech.*, **7**(3), 259-276.
- Hetenyi, M. (1946), *Beams on Elastic Foundation*, University of Michigan, Ann Arbor.
- Kerr, A.D. (1976), "On the derivation of well posed boundary value problems in structural mechanics", *Int. J. Solids Struct.*, **12**, 1-11.
- Kim, Y. and Jeong, S. (2011), "Analysis of soil resistance on laterally loaded piles based on 3D soil-pile interaction", *Comput. Geotech.*, **38**, 248-257.
- Kobayashi, N., Shibata, T., Kikuchi, Y. and Murakami, A. (2008), "Estimation of horizontal subgrade reaction coefficient by inverse analysis", *Comput. Geotech.*, **35**(4), 616-626.
- Setiadji, B.H., Fwa, T.F. (2009), "Examining k-E relationship of pavement subgrade based on load-deflection consideration", *J. Transp. Eng.-ASCE*, **135**(3), 140-148.
- Zhaohua, F. and Cook, R.D. (1983), "Beam elements on two-parameter elastic foundations", *J. Eng. Mech.-ASCE*, **109**(6), 1390-1402.